Forward nuclear glory in $^{12}C+^{12}C$ scattering

A. N. Ostrowski, W. Tiereth,* and H. Voit

Physikalisches Institut der Universität Erlangen-Nürnberg, D-8520 Erlangen, Germany

Very precise elastic cross sections have been measured in a very forward angular range (up to 1.6° laboratory) for the $^{12}C+^{12}C$ system at six energies not too far above the Coulomb barrier. From these data the symmetrized nuclear scattering amplitude $f_N^s(\theta)$ for small angles and the total reaction cross section σ_R could be derived making use of the generalized optical theorem for charged particles. It was found that $|f_N^s(0)|$ exceeds zero significantly in all cases investigated. This means that a forward nuclear glory exists in the $^{12}C+^{12}C$ scattering. This is the first time that evidence for a forward nuclear glory is deduced from experimental data.

I. INTRODUCTION

Originally the glory is a celestial phenomenon. Like the rainbow it is due to the scattering of sunlight by waterdroplets of a cloud. An observer may see the glory if he looks in such a way at the cloud that his shadow is projected onto it. Then he may have the beautiful, but also somehow elusive, vision of his shadow surrounded by a series of concentric rings of color. The existence of these rings indicates that an enhancement of the intensity of the scattered sunlight occurs in the backward direction. The normal glory is, therefore, actually a backward glory as contrasted by a forward glory which is characterized by an enhancement in the forward direction. The latter is the subject of the present work.

Nussenzveig and Wiscombe [1] have pointed out that the forward optical glory should be observable if visible light is scattered by spheres of dense liquids (water excluded) and certain glasses with suitable refractive indices. They explain the forward glory as an interference process between forward glory rays and the forward diffraction peak. The former originate from rays which impinge tangentially onto the sphere and which are subsequently critically reflected several times until they emerge finally as surface waves in the forward direction. The interference gives rise to an oscillatory behavior of the scattered intensity as a function of the wave number of the light (for fixed radius of the sphere). These oscillations are called glory undulations and can be considered as a fingerprint of the forward glory.

Due to the wave character of fast-moving atoms and nuclei one may expect that the forward glory shows up also in atom-atom and nucleus-nucleus collisions. In fact, the forward glory predicted by Bernstein [2] for atomic collisions has already been observed experimentally [3].

The situation was different for the nucleus-nucleus collision. Stimulated by the work of Nussenzveig and Wiscombe [1] on the optical analog, the possible existence of the forward nuclear glory in heavy-ion scattering as well as its observation by means of the optical theorem was discussed by Hussein et al. [4] some time ago. Moreover, the forward glory was predicted to exist

in heavy-ion encounters by Barrette and Alamanos [5] and Tiereth et al. [6]. Their prediction was based on analyses performed with synthetic or semisynthetic data, respectively. These analyses as well as the work of Hnizdo [7] showed, however, that a proof would only be possible if an unusual accuracy of the scattering data can be achieved. This is obvious because the forward glory represents always only a modest portion of the intensity scattered into the forward direction compared with the dominant Coulomb contribution. Therefore, a direct proof of the forward nuclear glory, based on real experimental data, was missing so far. In this paper this proof is given for the $^{12}C+^{12}C$ scattering system. Preliminary results of the present investigation have been given already in Ref. [8].

II. GENERALIZED OPTICAL THEOREM

The proof that a forward nuclear glory exists is strongly related to the ability to determine the nuclear scattering amplitude $f_N(\theta)$ at small scattering angles θ: A nonvanishing amplitude at $\theta \rightarrow 0°$ is evidence for a forward nuclear glory. Besides this it has been shown in the realm of the semiclassical scattering theory [9,10] that $|f_N(\theta)|$ exhibits an undulating envelope at forward angles if a forward glory exists. Thus the existence of a glory can only be established if $|f_N(\theta)|$ can be determined in a model-independent way at small angles. This can be achieved by means of the generalized optical theorem (GOT) for charged particles if sufficiently accurate experimental data are available in this angular range. Thus the GOT plays a crucial role for the detection of the nuclear forward glory as well as the experimental ability to take high-precision data.

The GOT for nonidentical spinless particles was first introduced by Holdeman and Thaler [11] to extend the normal optical theorem to the scattering of charged particles. The authors derived an expression which is only valid without approximations if screening effects are included in the calculation of the Coulomb cross section which enters into the expression for the GOT. Since the screening is difficult to take into account accurately the GOT of Ref. [11] has only limited value from the experi-

mental point of view.

Fortunately a very elegant formulation for the GOT has been given by Marty [12] and in a different way also by Lipperheide [13] which is valid without any approximations and makes simultaneously no recourse to the Coulomb screening. This version of the GOT connects the measurable quantity $\sigma_{SOD}(\theta_0)$ called sum-of-differences (SOD) cross section with the total reaction cross section σ_R and both the amplitude $|f_N(0)|$ and the phase $\phi_N(0)$ of the nuclear scattering amplitude at $\theta=0°$ in the following way:

$$\sigma_{SOD}(\theta_0)=\sigma_R-\frac{4\pi}{k}|f_N(0)|$$

$$\times \sin[\phi_N(0)-2\sigma_0$$

$$+2\eta \ln(\sin\tfrac{1}{2}\theta_0)]+C(\theta_0) , \qquad (1)$$

with k, σ_0, and η being the wave number, the s-wave Coulomb phase shift, and the Sommerfeld parameter, respectively. The angle θ_0 enters into Eq. (1) via the definition of the sum-of-differences cross section

$$\sigma_{SOD}(\theta_0):=2\pi\int_{\theta_0}^{\pi}[\sigma_C(\theta)-\sigma_{el}(\theta)]\sin\theta\, d\theta , \qquad (2)$$

where $\sigma_C(\theta)$ and $\sigma_{el}(\theta)$ are the differential Coulomb cross section and the measured elastic cross section, respectively. The quantity $C(\theta_0)$ is given by the following expression:

$$C(\theta_0)=2\pi\int_0^{\theta_0}|f_N(\theta)|^2\sin\theta\, d\theta$$

$$+4\pi\,\mathrm{Re}\left[\int_0^{\theta_0}f_C^*(\theta)[f_N(\theta)-f_N(0)]\sin\theta\, d\theta\right] , \qquad (3)$$

with $f_C(\theta)$ being the Coulomb scattering amplitude.

It is obvious that $C(\theta_0)$ can be neglected in the limit $\theta_0\to 0°$. This means that the measurable quantity $\sigma_{SOD}(\theta_0)$ has to oscillate at very small angles with constant amplitude $4\pi|f_N(0)|/k$ symmetrically with respect to the total reaction cross section σ_R. This feature of $\sigma_{SOD}(\theta_0)$ allows us to deduce $|f_N(0)|$ and also σ_R in a model-independent way provided that accurate $\sigma_{el}(\theta)$ values have been measured at very forward angles. As was pointed out already $|f_N(0)|$ is a measure of the nuclear forward glory.

It will be demonstrated below that the angular range in which $\sigma_{SOD}(\theta_0)$ oscillates with constant amplitude [i.e., the range where $C(\theta_0)=0$] is restricted to extremely small angles which are hardly accessible to a real experiment. It has been shown, however, by Barrette and Alamanos [5] that the GOT of Eq. (1) can be modified without any approximation so that the determination of the nuclear scattering amplitude is feasible with scattering data which do not have to extend into the angular range for which $C(\theta_0)=0$ holds.

The expression for the modified GOT is

$$\sigma_{SOD}(\theta_0)=\sigma_R-\frac{4\pi}{k}|f_N(\theta_0)|$$

$$\times \sin[\phi_N(\theta_0)-2\sigma_0$$

$$+2\eta \ln(\sin\tfrac{1}{2}\theta_0)]+C'(\theta_0) \qquad (4)$$

with

$$C'(\theta_0)=2\pi\int_0^{\theta_0}|f_N(\theta)|^2\sin\theta\, d\theta$$

$$+\frac{4\pi}{\eta}\mathrm{Im}\left[\int_0^{\theta_0}f_C^*(\theta)\frac{d\,f_N(\theta)}{d\theta}(1-\cos\theta)d\theta\right] .$$

It is important to note that $C'(\theta_0)$ can be safely skipped within a forward angular range which extends to much larger angles than the angular range in which $C(\theta_0)$ of Eq. (1) can be set zero. This means, indeed, that $|f_N(\theta)|$ can be determined from elastic data which extend to less forward angles.

From Eq. (4) it is obvious that $\sigma_{SOD}(\theta_0)$ oscillates symmetrically with respect to σ_R in the angular range where $C'(\theta_0)$ can be neglected. The oscillations do, however, not occur with constant amplitude [unless $|f_N(\theta)|$ is constant for small angles]. According to the semiclassical scattering theory one expects that the envelope of these oscillations behaves like the Bessel function $J_0(l_g\sin\theta)$ if a forward nuclear glory exists. It has been shown in the framework of this theory [9,10] that the absolute value of the scattering amplitude at forward angles θ ($\theta\leq\theta_g$, the angle of the first minimum of the Bessel function called glory minimum) can be expressed as

$$|f(\theta)|=|f(0)|J_0(l_g\sin\theta) , \qquad (5)$$

with l_g being the glory angular momentum which is expected to be close to the grazing angular momentum in the case of heavy-ion scattering. Thus an undulating envelope for $\sigma_{SOD}(\theta_0)$ also indicates the existence of a forward nuclear glory. This has been pointed out already in Ref. [5]. Obviously an undulating envelope can only be observed, however, if the glory angular momentum of the system studied is large enough to place the glory minimum into the angular range where $C'(\theta_0)\approx 0$. In the presence of a glory Eq. (5) can be used to extrapolate $|f_N(\theta)|$ determined with Eq. (4) to zero degrees.

Since the ^{12}C$+$^{12}C scattering system was investigated in the present work in search of a possible forward nuclear glory, the expressions given above have to be changed in order to account for the identity of the scattered spinless particles. The sum-of-differences cross section is now defined as

$$\sigma_{SOD}(\theta_0):=2\pi\int_{\theta_0}^{\pi/2}[\sigma_M(\theta)-\sigma_{el}(\theta)]\sin\theta\, d\theta , \qquad (6)$$

where $\sigma_M(\theta)$ is the differential Mott cross section. The two versions of the GOT given above [Eqs. (1) and (4)] have to be rewritten in the following way:

$$\sigma_{SOD}(\theta_0) \approx \sigma_R - \frac{4\pi}{k} |f_N^s(\alpha)| \{\sin[\phi_N^s(\alpha) - 2\sigma_0] + 2\cos[\varphi_N^s(\alpha) - 2\sigma_0 + \eta \ln(\sin\frac{1}{2}\theta_0)]\sin[\eta \ln(\tan\frac{1}{2}\theta_0)]\} , \qquad (7)$$

where α equals either $0°$ or θ_0. In (7) the symmetrized nuclear scattering amplitude $f_N^s(\alpha)$ shows up which is defined in the case of the $^{12}C + ^{12}C$ system as $f_N^s(\alpha) = f_N(\alpha) + f_N(\pi - \alpha)$.

The sum-of-differences cross section is only approximately equal to the right-hand side of (7) because the expressions analogue to $C(\theta_0)$ and $C'(\theta_0)$ are not written down explicitly [they are identical with $C(\theta_0)$ and $C'(\theta_0)$ given above if $f_N(\theta)$ is replaced by $f_N^s(\theta)$]. As in the case of nonidentical particles both approximations are, however, very good in the forward angular range which extends to larger angles if $\alpha = \theta_0$.

It is worthwhile to note that approximation (7) with $\alpha = 0°$ can be replaced in the limit $\theta_0 \to 0°$ by

$$\sigma_{SOD}(\theta_0) \approx \sigma_R - \frac{4\pi}{k} |f_N^s(0)| \sin[\varphi_N^s(0) - 2\sigma_0 + 2\eta \ln(\sin\frac{1}{2}\theta_0)] . \qquad (8)$$

This expression is identical with the GOT for nonidentical particles if $f_N(0)$ is replaced by the symmetrized form $f_N^s(0)$. With approximation (8) it is possible to determine $f_N^s(0)$ and σ_R for identical particles in a very simple and model-independent way provided that experimental data are available which cover the angular range for which approximation (8) is valid. σ_R can be identified with the mean value of the symmetric $\sigma_{SOD}(\theta_0)$ oscillations and $4\pi|f_N^s(0)|/k$ with the difference between the extrema of these oscillations and σ_R.

Both quantities can, however, also be determined without applying a model if the data cover the angular range for which (7) with $\alpha = \theta_0$ is a good approximation. In this case σ_R can be evaluated by means of the upper and lower envelopes connecting the extrema of the $\sigma_{SOD}(\theta_0)$ oscillations; i.e., σ_R can be associated with the value given by the intersection of the median of both envelopes with the ordinate. $|f_N^s(\theta)|$ and $\phi_N^s(\theta)$ have to be adjusted according to (7) to fit the measured $\sigma_{SOD}(\theta_0)$.

III. EXPERIMENTAL REQUIREMENTS

In the following section the requirements are discussed which have to be met by the experiment to be able to deduce reliable values for σ_R and $f_N^s(\theta)$ from elastic-scattering data by means of the GOT. These requirements have a direct impact on the experimental setup. The most crucial point is how far toward forward angles and in which angular steps the measurements have to be performed. Of similar importance is the influence of a number of experimental errors (statistical error, normalization error, errors from the incorrect knowledge of the scattering angle, errors from target contaminations) which will be also discussed. The discussion is based on an analysis of semisynthetic elastic data of the $^{12}C + ^{12}C$ system.

The $^{12}C + ^{12}C$ system was chosen for the present investigations for two reasons: (i) a forward nuclear glory was predicted by Hussein et al. [14] for $^{12}C + ^{12}C$ and (ii) there exist already very reliable elastic data for $^{12}C + ^{12}C$ which were measured in the angular range $20° < \theta_{c.m.} < 90°$ by Treu et al. [15]. Besides this, the availability of very thin targets was an additional argument in favor of the $^{12}C + ^{12}C$ system.

A. Angular range, angular steps

Figure 1 shows the sum-of-differences cross section $\sigma_{SOD}(\theta_0)$ (solid line) as calculated with Eq. (6) from a semisynthetic elastic angular distribution for $^{12}C + ^{12}C$ at $E_{c.m.} = 9.5$ MeV. The latter was generated from S-matrix elements which were obtained from a phase-shift analysis of the experimental data of Treu et al. [15]. The figure also shows $\sigma_{SOD}(\theta_0)$ as calculated by means of the approximations (7) and (8) (dotted and dashed lines, respectively). For approximation (7) $\alpha = \theta_0$ was used. Obviously, (8) is a good approximation in the angular range $0° < \theta_0 \leq 4°$. This means that $|f_N^s(0)|$ and σ_R can be easily deduced from $\sigma_{SOD}(\theta_0)$ if the measured elastic data extend to angles $\theta_0 < 4°$. In fact, the median of the forward oscillations in Fig. 1 intersects the ordinate at a value which corresponds exactly to σ_R as calculated from the S-matrix elements. Similarly, if $4\pi|f_N^s(0)|/k$ is deduced from Fig. 1 as the difference between an extremum of the forward oscillations and σ_R one obtains also the S-matrix value.
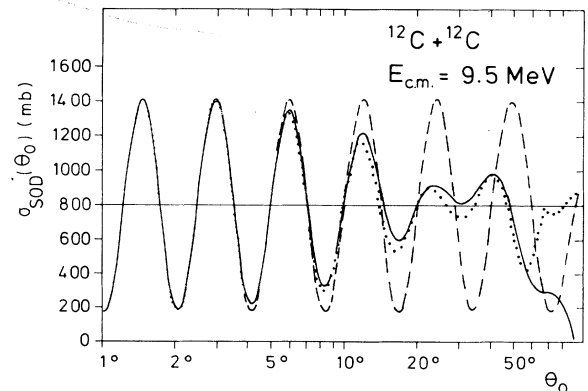
Figure 1 shows furthermore that approximation (7) is

FIG. 1. Sum-of-differences cross section $\sigma_{SOD}(\theta_0)$ (solid line) calculated by means of Eq. (6) from semisynthetic elastic data (see text) for the $^{12}C + ^{12}C$ scattering at $E_{c.m.} = 9.5$ MeV. The dotted and dashed lines represent calculations for $\sigma_{SOD}(\theta_0)$ by means of approximations (7) and (8), respectively. The horizontal line represents the median of the upper and lower envelopes through the σ_{SOD} oscillations.

valid for angles $\theta_0 \leq 10°$. Thus, an angular distribution measured until $\theta_0 = 5°$ (or 2.5° in the laboratory system) would be already sufficient to deduce both quantities $|f_N^s(\theta)|$ and σ_R in a model-independent way as discussed in Sec. II.

From Fig. 1 it is easy to see that the elastic angular distribution has to be measured in very small angular steps $\Delta\theta$ at forward angles in order to pin down the σ_{SOD} oscillations. With the assumption that at least six data points are necessary to identify one period needed to construct the upper and lower envelopes one finds $\Delta\theta \approx 0.5°$ for the angular range $3° < \theta < 10°$. This small angular increment as well as the extremely small scattering angles represent a considerable challenge for the experimentalist.

B. Normalization

The effect of an incorrect overall normalization of the elastic data can be seen from Fig. 2 which shows $\sigma_{SOD}(\theta_0)$ as calculated from correct data (solid line), and from data which were multiplied by an arbitrary factor, i.e., from data with an incorrect absolute normalization (dotted and dashed lines). The latter yield $\sigma_{SOD}(\theta_0)$ functions with medians for the upper and lower envelopes which have a finite slope. Since the median is related to σ_R according to the GOT one expects, however, a horizontal line for correctly normalized data. One can use this prediction of the GOT, on the other hand, in order to find the correct normalization for the data.

C. Statistical error

The influence of the statistical error of the data points on the proposed investigation was also studied by means of the synthetic ^{12}C+^{12}C data at $E_{c.m.} = 9.5$ MeV. First of all it was assumed that the synthetic angular distribution consists of data points which have a statistical error which increases with the scattering angle in proportion to the decrease of the Coulomb cross section. Then each
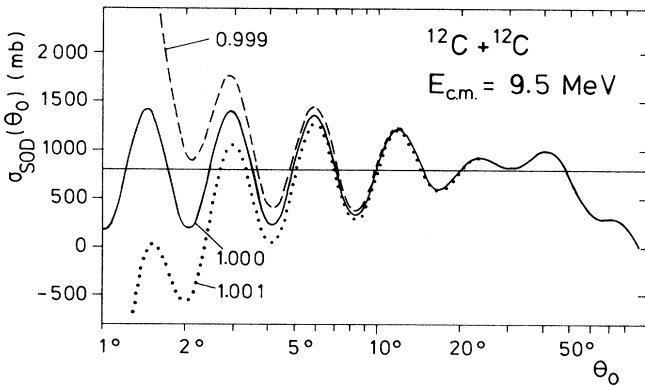
data point was placed randomly within the error bar. From these data points $\sigma_{SOD}(\theta_0)$ was generated. The relative error of the smallest angle used for this investigation $(\theta_{c.m.} = 3°)$ was varied systematically. It turned out that the relative statistical error for the data point at 3° has to be considerably smaller than 0.5%. Otherwise a completely erratic behavior of the deduced $\sigma_{SOD}(\theta)$ curves is obtained at small angles.

The effect of the statistical error on the reliability of the deduced $|f_N^s(\theta)|$ and σ_R values was investigated along the lines given by Marty [16] who has shown that the statistical error introduces an error $\delta\sigma_{SOD}(\theta_0)$ to $\sigma_{SOD}(\theta_0)$. $\delta\sigma_{SOD}$ is given by

$$\delta\sigma_{SOD}(\theta_0 = \theta^J) = \left[\sum_{K=J}^{M} (\delta H_K)^2 \right]^{1/2} , \tag{9}$$

provided that a sufficient number of data points has been measured at the angles θ^K $(K = J+1, \ldots, M-1; \theta^J = \theta_0$ and $\theta^M = 90°)$. δH_K is obtained by means of the trapezoidal rule as

$$\delta H_K = (\theta^{K+1} - \theta^{K-1})\delta I(\theta^K)/2 ,$$

$$\delta H_J = (\theta^{J+1} - \theta^J)\delta I(\theta^J)/2 ,$$

$$\delta H_M = (\theta^M - \theta^{M-1})\delta I(\theta^M)/2 ,$$

with $\delta I(\theta^K)$ being the error of the integrand of Eq. (6), i.e., $\delta I(\theta^K) = 2\pi[\Delta\sigma_{el}(\theta^K)\sin\theta^K]^{1/2}$, where $\Delta\sigma_{el}(\theta^K)$ is the statistical error of the measured elastic cross section. For the evaluation of $\delta I(\theta^K)$ it is assumed that the scattering angle θ^K is known exactly.

Figure 3 shows the curves $\sigma_{SOD}(\theta_0) \pm \delta\sigma_{SOD}(\theta_0)$ with $\delta\sigma_{SOD}(\theta_0)$ calculated according to Eq. (9). For this calculation it was assumed that $N(3°) = 10^5$ [$N(3°)$ is the number of counts at $\theta_{c.m.} = 3°$] and that $N(\theta^K)$ decreases for $\theta^K > 3°$ with increasing angles according to the de-

FIG. 2. Sum-of-differences cross section $\sigma_{SOD}(\theta_0)$ as computed with Eq. (6) from correctly normalized synthetic data (solid line) and from data with an incorrect overall normalization (dashed and dotted lines). The numbers in front of the curves indicate the factors which were used to multiply the correct data.
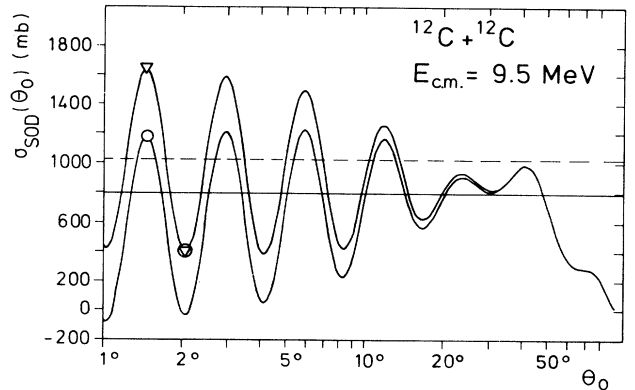

FIG. 3. Upper and lower values for $\sigma_{SOD}(\theta_0)$ obtained from data with a given statistical error (see text). The actual σ_{SOD} values are distributed between the two lines. The solid horizontal line indicates the correct σ_R value. The dashed line indicates the σ_R value which exceeds the correct value by the largest possible amount. For the meaning of the circles and triangles see text.

crease of the Mott cross section until a value of $N(\theta^K) = 10^3$ is reached which is then kept constant for still larger angles. This choice is relevant to an experimental setup where identical solid angles are chosen for the most forward scattering angles and where $N(\theta^K)$ always exceeds 10^3.

The actual experimental data points will be statistically distributed between the solid lines of Fig. 3. If a sufficient number of data points is measured within an angular range which exhibits a few $\sigma_{SOD}(\theta_0)$ oscillations, one will be able to construct the upper and lower envelopes to $\sigma_{SOD}(\theta_0)$ and thus the median which in turn gives the correct σ_R value.

Actually only a limited angular range with a few data points and one to two oscillations will be available. In the worst case the data points are distributed as indicated by the triangles in Fig. 3. This results in a σ_R value (upper dashed line in Fig. 3) which exceeds the correct σ_R (solid line). Similarly a too small σ_R value is obtained if the data points fall onto the extrema of the function $\sigma_{SOD}(\theta_0) - \delta\sigma_{SOD}(\theta_0)$. Thus σ_R is only known within the limits $\sigma_R \pm \delta\sigma_{SOD}(\theta_0)$, where θ_0 belongs to the most forward angular range.

The largest error for the $|f_N^s(\theta)|$ determination arises if the data points are distributed as indicated by the circles in Fig. 3. In this case a $|f_N^s(\theta)|$ value is obtained which is smaller than the correct value. Similarly $|f_N^s(\theta)|$ is too large if the data points coincide with a maximum and the subsequent minimum of the $\sigma_{SOD} + \delta\sigma_{SOD}$ and $\sigma_{SOD} - \delta\sigma_{SOD}$ curves, respectively. Again, the error $\Delta|f_N^s(\theta)|$ is related in a simple way to $\delta\sigma_{SOD}(\theta_0)$.

The example discussed yields relative errors of 24% and 34% for σ_R and $|f_N^s(\theta)|$, respectively. These errors can be decreased considerably if the number of counts $N(\theta)$ exhibits the same angular dependence as above with $N(3°) = 10^7$, i.e., a relative statistical error of 0.03% at the most forward angles. With this high statistical accuracy one obtains relative errors of 3.8% and 4.9% for σ_R and $|f_N^s(\theta)|$, respectively. This order of magnitude for the relative errors was aspired for the experimental data. Moreover, the experiment was arranged in such a way that the statistical error was the dominating error. Contributions to the experimental error from other sources (uncertainties in the scattering angle, target contaminations) were kept below the 0.03% limit.

D. Scattering angle

The accurate knowledge of the exact scattering angle is most important for a successful glory experiment. To illustrate this, four $\sigma_{SOD}(\theta_0)$ curves were calculated from the synthetic elastic data at $E_{c.m.} = 9.5$ MeV exhibiting a systematic angular shift of $\pm 0.01°$ and $\pm 0.001°$. These angular shifts can be partially corrected for using a renormalization of the data with an appropriate factor (0.9900 and 0.9225, respectively). In order to make the remaining deviation from the correct $\sigma_{SOD}(\theta_0)$ curve visible the differences $\Delta\sigma_{SOD}(\theta_0)$ between the correct and the incorrect curves are shown in Fig. 4(a) (dotted and dashed curves).

The figure also shows $\Delta\sigma_{SOD}(\theta_0)$ curves (solid lines)

which represent the differences between the exact $\sigma_{SOD}(\theta_0)$ and the functions $\sigma_{SOD}(\theta_0) \pm \delta\sigma_{SOD}$ from data which exhibit the statistical errors tolerated for the present experiment (0.03% at the most forward angles; see preceding section). The difference $2\delta\sigma_{SOD}$ between the solid curves of Fig. 4(a) is directly related to $\Delta\sigma_R$ ($\Delta\sigma_R = \delta\sigma_{SOD}$) and $\Delta|f_N^s(\theta)|$. It defines an error band which results exclusively from the statistical errors of the elastic data. Actually the difference at $\theta_0 \lesssim 5°$ is relevant since a model-independent determination of σ_R and $|f_N^s(\theta)|$ is only possible if the data extend to angles $\theta_0 \lesssim 5°$ as has been shown above.

Since it was desired to keep all other errors smaller than the statistical error given above, one had to require that the $\Delta\sigma_{SOD}$ curves obtained from data which contain errors different from the statistical error remain well within the error band introduced above. Obviously, this requirement is only fulfilled for the 0.001° curve as can be seen from Fig. 4(a). This means that the scattering angles should be known with an accuracy of 0.001° in the present glory experiment at the most forward angles.

E. Target contaminations

The analysis of the ^{12}C targets used in the present experiment showed that the following contaminations are

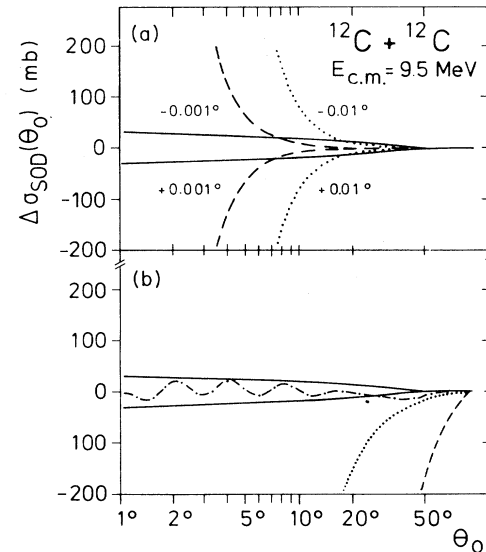FIG. 4. (a) Influence of a systematic angular shift on the σ_{SOD} function: the solid line shows the difference $\Delta\sigma_{SOD}(\theta_0)$ between the exact $\sigma_{SOD}(\theta_0)$ and $\sigma_{SOD}(\theta_0) \pm \delta\sigma_{SOD}$ as obtained from data which exhibit a statistical error $[N(3°) = 10^7$; see text]. The dotted and dashed curves represent the differences $\Delta\sigma_{SOD}(\theta_0)$ between the exact $\sigma_{SOD}(\theta_0)$ and $\sigma_{SOD}(\theta_0)$ calculated from scattering data which exhibit angular shifts of $\pm 0.01°$ and $\pm 0.001°$, respectively (+ means toward the beam direction). (b) Influence of target contaminations on $\sigma_{SOD}(\theta_0)$. The solid lines are the $\Delta\sigma_{SOD}$ functions of part (a). The dashed line represents the difference between the exact $\sigma_{SOD}(\theta_0)$ and $\sigma_{SOD}(\theta)$ obtained from data which were not corrected for the typical target contaminations (for details see text). The dotted and dash-dotted lines show $\Delta\sigma_{SOD}$ after correction for the target contaminations and an additional renormalization, respectively.

typically present: 1.1% ^{13}C, 5% ^{16}O, 0.1% ^{56}Fe, and 0.01% ^{197}Au. In order to study the influence of these contaminations an elastic angular distribution was synthesized containing contributions from the elastic scattering of ^{12}C on ^{12}C and from the above contaminations. The latter contributions were calculated assuming pure Rutherford scattering. The difference $\Delta\sigma_{\text{SOD}}(\theta_0)$ between $\sigma_{\text{SOD}}(\theta_0)$ obtained from this angular distribution and the exact $\sigma_{\text{SOD}}(\theta_0)$ (assuming a pure ^{12}C target) is shown as the dashed curve in Fig. 4(b). Also shown are the two $\Delta\sigma_{\text{SOD}}(\theta_0)$ curves (solid lines) of Fig. 4(a) which result from elastic data with a relative statistical error of 0.03% at forward angles.

Obviously, the contributions from the contaminations have to be taken into account in order to keep the resulting error small. This has been done in the following way: (i) 90% of the contributions from the contaminations were subtracted and (ii) the resulting $\sigma_{\text{SOD}}(\theta_0)$ was renormalized using the symmetry criterion for the σ_{SOD} oscillation. The differences $\Delta\sigma_{\text{SOD}}(\theta_0)$ of the resulting $\sigma_{\text{SOD}}(\theta_0)$ curves and the exact $\sigma_{\text{SOD}}(\theta_0)$ are shown in Fig. 4(b) as dotted [only procedure (i)] and dash-dotted [procedures (i) and (ii)] lines. $\Delta\sigma_{\text{SOD}}(\theta_0)$ obtained from procedures (i) and (ii) does not leave the error band given by the two solid lines in the forward angular range. This means that the subtraction of the contributions from target contaminations yields useful $\sigma_{\text{SOD}}(\theta_0)$ functions provided that the percentage of the contaminations is known with an accuracy of $\leq 10\%$.

The investigations of Sec. III clearly show that the glory angular distributions has to be measured to forward angles as small as $\theta_{\text{c.m.}} = 5°$ (better 3°) in angular steps of 0.5°. The relative statistical error at the smallest angles should be $\leq 0.03\%$ to get reliable $|f_N^s(\theta)|$ and σ_R values. If it is requested that this error gives the largest contribution to the total error of $|f_N^s(\theta)|$ and σ_R, one needs in addition an angular accuracy of 0.001° at the most forward angles; besides this the percentage of the target contaminations must be known with an accuracy of $\leq 10\%$.

IV. EXPERIMENTAL SETUP AND PROCEDURE

A. Scattering chamber

For the glory experiment a trapezoidal scattering chamber was built. This chamber is shown in Fig. 5. At the front end it is connected to the target chamber which houses the target ladder with seven target positions. At the rear end the movable slit system and the detector chamber is mounted. The distance between target and slit position is 1453 mm. 10 mm in the direction of the slit system correspond to an angular increment of 0.4° as a consequence of this large distance.

The slit system consists of a movable frame on which a 0.1-mm-thick Ni strip is fixed. The position of the frame can be changed within 25 mm with an accuracy of 10 μm. The Ni strip contains 36 slits with the dimension 8 mm$\times$0.4 mm and an angular distance of 0.4° with the exception of the slits 2 and 3 which exhibit a distance of 4.8° (the slits are numbered from right to left with respect to the beam direction). The slits were manufactured by means of electroerosion.

The linear distance of the slits was determined with an accuracy of 25 μm by means of a milling machine (5-μm accuracy) and a laser-photodiode system. The relative solid angles of the first four slits were determined using an α-particle source and a surface barrier detector. The number of α-particles passing through the slits is a very sensitive measure of the relative solid angles.

With the accurate knowledge of the relative solid angles of slits 2 and 3 it is possible to determine the beam position very accurately. Beam position, linear distance between the slits, and the precisely known distance between target and slit allow a determination of the geometrical scattering angles θ of the detector. With the knowledge of the scattering angles it is possible to determine, in turn, the relative solid angles of the slits by means of a low-energy scattering experiment (elastic scattering of ^{12}C+^{12}C at $E_{\text{c.m.}} = 4$ MeV).

It should be noted that the geometrical scattering angles θ and the solid angles $d\Omega^*$ determined in this way coincide with the actual scattering angles θ_a and the real solid angles $d\Omega$ only if the beam divergence D is negligibly small. A finite beam divergence results in a shift of θ_a to smaller angles relative to θ due to the strong increase of the Mott cross section at forward angles. This shift also depends on the actual beam profile. In addition, the relative solid angles $d\Omega^*$ determined from the low-energy measurement differ from $d\Omega$ by a factor f which is given by the ratio of the Mott cross sections for θ_a and θ, respectively.

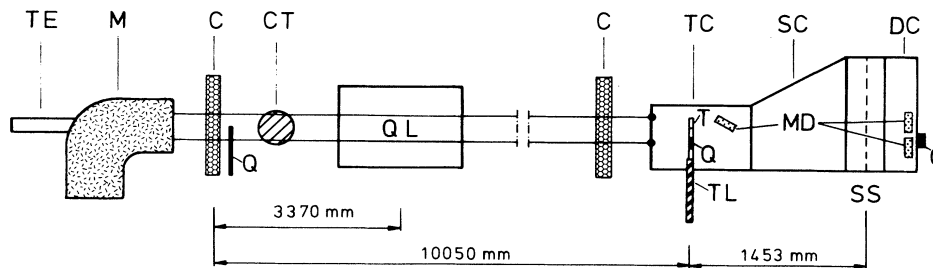The shift between θ_a and θ increases at forward angles

FIG. 5. Schematics of the experimental setup: M=90° analyzing magnet, TE=telescope, C=collimator wheel, CT=cold trap, QL=quadrupole lense, TC=target chamber, SC=scattering chamber, DC=detector chamber, T=target, TL=target ladder, SS=slit system, MD=monitor detector, Q=beam viewer.

and gives rise to an angle-dependent systematic error of the measured cross sections if the real solid angles $d\Omega$ are used for the normalization. In this case the systematic error can only be partially corrected for by the normalization procedure described in Sec. III B.

In the present case ($D \leq 0.1°$, Gaussian beam profile) one obtains angle shifts of the order of $0.008°$ at the smallest angles. From these shifts relative errors of the measured cross sections as large as 1% would result. The angle shifts decrease below $0.001°$ (the value discussed in Sec. III D) no sooner than $\theta \geq 10°$.

Fortunately the angle shift does not really affect the present measurements. The reason is that the relative solid angles $d\Omega^*$ were used to normalize all measured angular distributions and since much care was taken to obtain the same beam divergence in all runs. The latter guarantees that identical (within the aspired angle accuracy) angle shifts occurred at all runs and that the solid angle factor f is nearly the same (within the aspired accuracy) for all energies investigated. Thus the normalization with $d\Omega^*$ gives cross sections which belong to the geometrical scattering angle θ. Note that the smallest angle contained in the present data belongs to the scattering through slit 4.

B. ^{12}C beam

The glory experiment was performed with the ^{12}C beam of the Erlangen EN tandem accelerator. Each beam line of this accelerator starts with a 90° analyzing magnet. This has the advantage that the experimental setup can be aligned very precisely by means of a telescope or a laser mounted on the rear side of the magnet (see Fig. 5). Moreover, the alignment can be checked permanently during the experiment. Much effort was used to obtain a ^{12}C beam with a very small beam divergence at the target. For this purpose the ion optics was optimized with the program TRANSPORT [17]. As a result of these calculations, the target chamber was placed at a rather large distance from the quadrupole lense (see Fig. 5). In this way a beam spot at the target with a diameter of less than 1.5 mm and a divergence $\leq 0.1°$ could be achieved.

C. ^{12}C targets

The ^{12}C targets were prepared from reactor graphite by means of electron beam evaporation. Target thicknesses as determined by means of the energy loss of α particles were 6 to 10 $\mu g\,cm^{-2}$. Target contaminations consisting of light- and medium-mass nuclei have been determined with an accuracy of less than 10%. The analysis was performed during and after (with reduced beam energy) the glory experiment by means of a Si detector which was placed in the target chamber at 27° with respect to the beam direction. Heavy-target contaminations were determined by means of an x-ray fluorescence analysis.

An increase of the ^{12}C thickness during the irradiation was not observed; likewise no visible beam spot was found at the targets after irradiation. This was due to the rather good vacuum in the target chamber ($<5\times10^{-7}$

mbar) and the very small beam intensity used during the measurement (≤ 100 pA).

D. Heavy-ion detector

It is essential for a high-precision scattering experiment to use a detector system which allows us to measure an almost complete angular distribution simultaneously in order to avoid normalization problems. In the present case a position-sensitive proportional counter (PSPC) was used in connection with the slit system described above. This system defines the scattering and the solid angles. It made no sense to use a more sophisticated detector which would have allowed us to discriminate between ^{12}C ejectiles scattered from ^{12}C and the target contaminations or between ^{12}C and recoil nuclei. In the first case the energy difference is too small to be measured with heavy-ion detectors available; in the second case one can safely argue that recoil contributions other than ^{12}C are negligibly small.

The PSPC consists of a u-shaped brass cathode with a resistive wire (620 mm long, 7.5 μm diameter, specific resistance 12 $\Omega\,m^{-1}$) stretched within. The counter is mounted in the detector chamber (see Fig. 5) which is filled with 40 Torr isobutan. The gas pressure was kept constant within ±1 Torr by means of a regulating system. A relatively large gas flow was maintained in order to avoid degradation of the counter gas. The detector chamber is separated from the scattering chamber by a 660×16-mm^2 window covered with a 1.5-μm-thick Mylar foil.

The detector chamber contains, in addition, two rectangular Si detectors mounted on a movable sledge. The distance between both detectors corresponds to the distance between slits 2 and 3. They were used to monitor scattering from the target frame which indicates a deterioration of the beam spot quality.

Position-sensitive signals were obtained from the PSPC using the charge division method [18]. A typical position spectrum obtained for the $^{12}C + ^{197}Au$ scattering at $E_{lab} = 12.8$ MeV is shown in Fig. 6. Here the split sys-
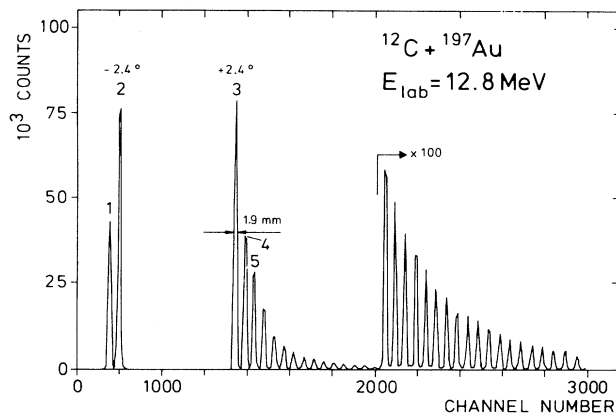

FIG. 6. Position spectrum of the elastic scattering of ^{12}C ($E_{lab} = 12.8$ MeV) on ^{197}Au. Some of the peaks are labeled with the numbers of the corresponding slits. The angular difference between successive slits is 0.4° with the exception of slits 2 and 3 which exhibit a distance of 4.8°.

tem was thus positioned that slits 2 and 3 were symmetrically arranged with respect to the ^{12}C beam.

Obviously, Fig. 6 shows that the position resolution of the PSPC is sufficient to take data in angular steps of 0.4° in the laboratory system (the angular difference between successive slits is 0.4°). It requires two runs to obtain one complete angular distribution with steps of less than 0.25° necessary according to the investigations of Sec. III A. For the second run the slit system was moved by 0.2°.

E. Experimental procedure

The ^{12}C+^{12}C elastic scattering at very forward angles has been measured at $E_{c.m.} = 6.38$, 7.08, 8.69, 9.48, 11.15, and 11.40 MeV. At 11.40 MeV a $J^{\pi} = 8^{+}$ resonance is known from previous investigations [15,19]. $E_{c.m.} = 6.38$ MeV is close to a $J^{\pi} = 4^{+}$ resonance at 6.4 MeV [19,20]. All other energies are off-resonance energies. The energies quoted are corrected for the energy loss in the ^{12}C target. The resonance energy was determined experimentally by means of the reaction ^{12}C(^{12}C,α_0)^{20}Ne, i.e., an excitation function was measured for this reaction at $\theta_{lab} = 18°$ in energy steps of 50 keV (laboratory) with a target of the same thickness used in the glory experiment. It is known from previous experiments [20] that the $\theta_{lab} = 18°$ excitation function of the α_0 exit channel exhibits a pronounced maximum at the resonance energy.

The ^{12}C beam was optimized very carefully before each of the elastic angular distributions was measured. First of all the beam was tuned in such a way that a small divergence ($\leq 0.1°$) and a tiny beam spot (diameter ≤ 1.5 mm) were obtained at the target. This was achieved with the aid of several quartz viewers exhibiting a 1-mm hole in the center. In the next step the slit system was brought into a precisely defined position with respect to the beam direction. For this purpose the scattering of ^{12}C on a thin ^{197}Au target measured behind slits 2 and 3 (with precisely known solid angles) was used. This procedure defines the actual scattering angles given by the slit system. Finally the energy spectra of the Si detectors behind slits 2 and 3 were examined as to scattering from the target frame.

During the actual measurement of the elastic data the counting rate of the Si monitors was both continuously monitored and accumulated within fixed time intervals in order to control the beam position. In the few cases where a marked deviation from the original position occurred, the beam was retuned and the data were erased. In case of small beam shifts the scattering angles were corrected. For this purpose the actual data were stored continuously after fixed time intervals. Each angular distribution was measured in two runs. For the second run the slit system was shifted by 0.2° with respect to the position used in the first run. The smallest angles for which data could be taken were $\theta_{lab} = 2.4°$ ($E_{c.m.} = 6.38-9.48$ MeV) and $\theta_{lab} = 1.6°$ ($E_{c.m.} = 11.15$ and 11.4 MeV), respectively. In both cases the smallest angle corresponds to slit 4. In each run more than 10^7 events were accumulated for the most forward angles.

The beam intensity was kept rather small (≤ 100 pA) during the actual measurement since it was found that the resistive wire is damaged by a high flux of scattered particles. The damage results in blind sections and a deterioration of the position resolution. The data collection time for one angular distribution was of the order of 24 h due to the small beam intensity and the small statistical error required.

V. EXPERIMENTAL RESULTS

A. Physical effects

Since the scattering data were measured with very high precision, it was necessary to check whether a number of small physical effects, normally not considered in the case of low-energy heavy-ion scattering, exercise an influence on the measured data. The effects to be considered are dynamical nuclear polarization, electron screening, small-angle multiple scattering, and vacuum polarization.

It has been shown by Vetterli et al. [21] that the dynamical nuclear polarization can be neglected in the ^{12}C+^{12}C scattering for impact parameters relevant in the present measurements. The electronic screening was discussed for the ^{12}C+^{12}C system by Assenbaum et al. [22]. From this work one can deduce that screening has to be considered only for impact parameters smaller than 8.8 pm (corresponding to $\theta_{lab} = 0.02°$) at the smallest projectile energy investigated.

The effect of the multiple scattering can be seen from Fig. 7 which shows the normalized probability distributions of the projected scattering angles θ for multiple and single scattering of ^{12}C+^{12}C at $E_{c.m.} = 10.0$ MeV. The former is calculated as [23]

$$P_M(\theta)d\theta = (\pi \langle \theta^2 \rangle)^{-1/2} \exp \left[\frac{-\theta^2}{\langle \theta^2 \rangle} \right] d\theta , \qquad (10)$$

with $\langle \theta^2 \rangle^{1/2}$ being the average scattering angle resulting from a large number of single-scattering events. The probability distribution $P_s(\theta)d\theta$ for single-scattering events can be easily deduced from Mott's scattering formula [23]. $\langle \theta^2 \rangle$ was calculated by means of a semiexperimental relation given in Refs. [24] and [25]. Obviously, the effect of the multiple scattering can be neglected for the smallest angles ($\theta_{c.m.} \geq 3.2°$) investigated in this work.
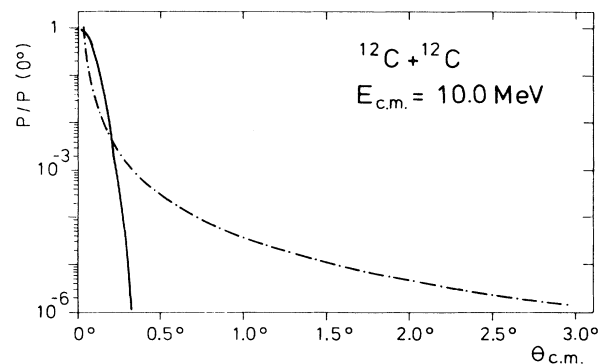

FIG. 7. Probability distributions for multiple- (solid line) and single-scattering (dashed line) events.

Figure 8 shows the effect of the vacuum polarization in terms of the ratio between the modified and the pure Mott cross sections $\sigma'_M(\theta)$ and $\sigma_M(\theta)$, respectively. For the calculation of $\sigma'_M(\theta)$ the vacuum polarization was taken into account as a first-order perturbation as proposed by Uehling [24] who showed that the modified scattering amplitude $f'_c(\theta)$ can be written as $f'_c(\theta) = f_c(\theta)[1 + \eta(\theta)]$ [the analytical expression for $\eta(\theta)$ can be found in the work of Uehling]. With Uehling's approximation one obtains $\sigma'_M(\theta)/\sigma_M(\theta) = [1 + \eta(\theta)]^2$ which is shown in Fig. 8 for the case of the $^{12}C + ^{12}C$ scattering at 6.4 MeV. Obviously the effect of the vacuum polarization is large enough to be seen in our data. Actually it shows up most clearly in σ_{SOD} functions which extend to very forward angles. This is due to the fact that the ratio σ'_M/σ_M increases rapidly with increasing θ in this angular range. The effect can hardly be seen in σ_{SOD} functions derived from elastic data measured only at larger angles where σ'_M/σ_M is nearly constant (see Fig. 8). In this case the vacuum polarization is masked by the normalization procedure. Since our data extend to very forward angles, the effect of the vacuum polarization has to be taken into account.
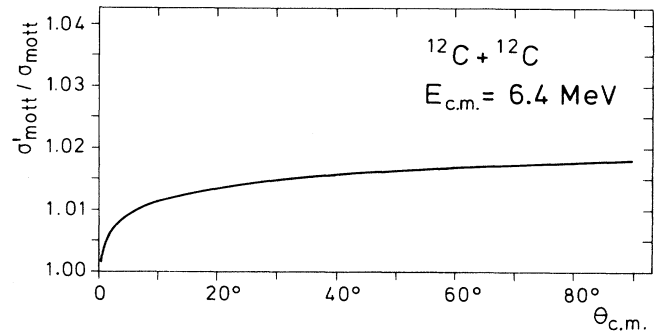

FIG. 8. Ratio between the Mott cross section calculated with (σ'_M) and without inclusion of the vacuum polarization [24].

B. Angular distributions

Angular distributions have been measured in the present work in the angular range $\theta_{c.m.} = 4.8°(3.2°) - 29°$ at energies for which very precise elastic data had been measured [15] already for angles $20° \leq \theta_{c.m.} \leq 90°$. The raw data were obtained in two runs differing in the posi-
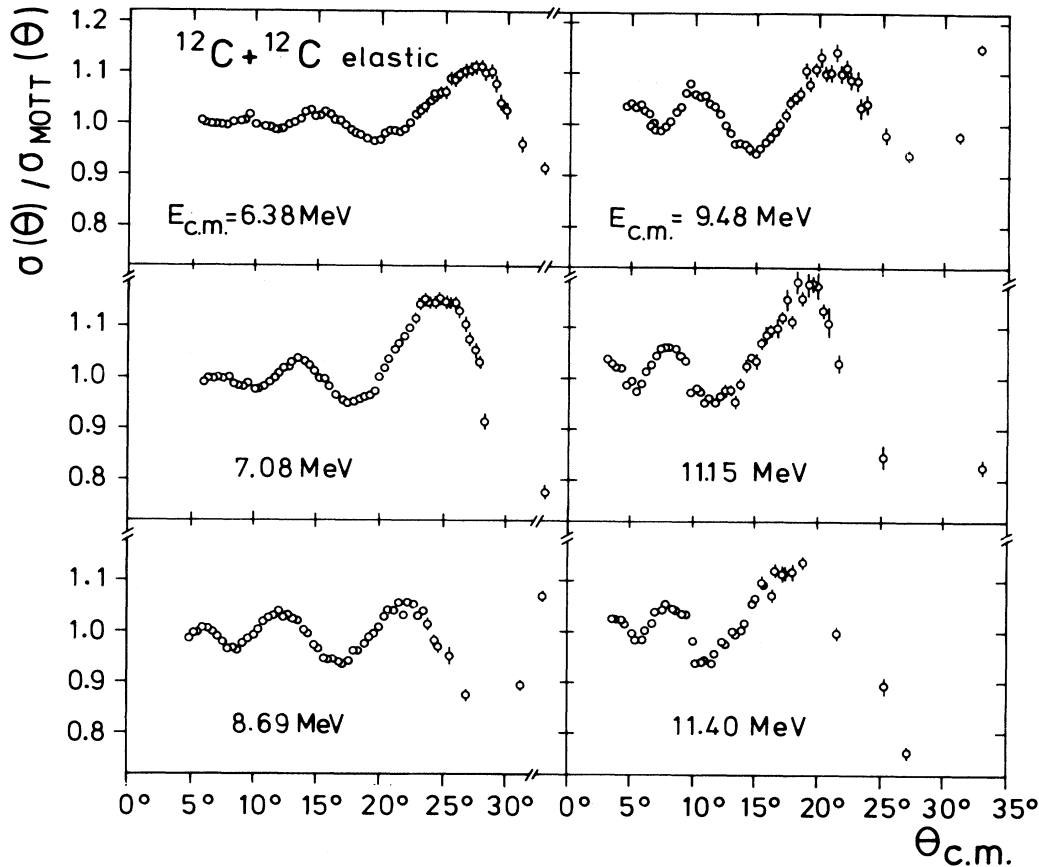

FIG. 9. Angular distributions of the elastic scattering $^{12}C + ^{12}C$ measured at $E_{c.m.} = 6.38$, 7.08, 8.69, 9.48, 11.15, and 11.40 MeV in the present work.

tion of the slit system by an angular shift of 0.4° (c.m.). They were corrected for contributions from target contaminations which were subtracted according to the corresponding Rutherford cross section and the percentage obtained for each contamination from the target analysis. The data of the two runs were adjusted to each other to give a smooth curve. Then they were normalized with respect to the Mott cross section (modified with respect to the vacuum polarization) in such a way that smooth oscillations around the value 1 were obtained for the ratio $\sigma_{el}(\theta)/\sigma_M(\theta)$. The final normalization was performed by means of the symmetry criterion for $\sigma_{SOD}(\theta_0)$ (see Sec. III B). Figure 9 shows the angular distributions obtained in this way. Figure 10 shows the complete angular distributions including the previously measured data [15] for large scattering angles.

C. Sum-of-differences cross sections

The sum-of-differences cross sections were calculated by means of Eq. (6) [with a modified $\sigma_M(\theta)$ to account for the effect of the vacuum polarization] from the measured angular distributions. The latter were approximated by means of a cubic spline function [25]. This spline approximation made it possible to carry out the integration of Eq. (6) in very fine angular steps [26]. The result-

ing $\sigma_{SOD}(\theta_0)$ functions were multiplied by a normalization factor which was chosen in such a way that the median of the upper and lower envelopes of $\sigma_{SOD}(\theta_0)$ became a horizontal line (see Sec. III B).

The $\sigma_{SOD}(\theta_0)$ distributions obtained in this way are shown in Fig. 11. The error bars were calculated according to Eq. (9). All $\sigma_{SOD}(\theta_0)$ functions exhibit oscillations at small angles. This is exactly the behavior expected from the analysis of the synthetic data performed in Sec. II.

It is worthwhile to note that the magnitude of the oscillations in the $\sigma_{SOD}(\theta_0)$ functions for $E_{c.m.} = 11.15$ and 11.40 MeV is quite different even though the angular distributions seem to be rather similar in both cases at first sight (see Figs. 9 and 10). A close inspection of Fig. 9 shows, however, that there are small differences in the absolute height of the cross sections at small angles where different amplitudes of the $\sigma_{SOD}(\theta_0)$ oscillations are observed. These small cross-section differences give rise to dramatic effects in the $\sigma_{SOD}(\theta_0)$ functions. The unusual accuracy required for the present experiments is particularly necessary to work out such differences.

VI. DISCUSSION

A first inspection of Fig. 11 shows already that almost all amplitudes of the σ_{SOD} oscillations are of the same or-
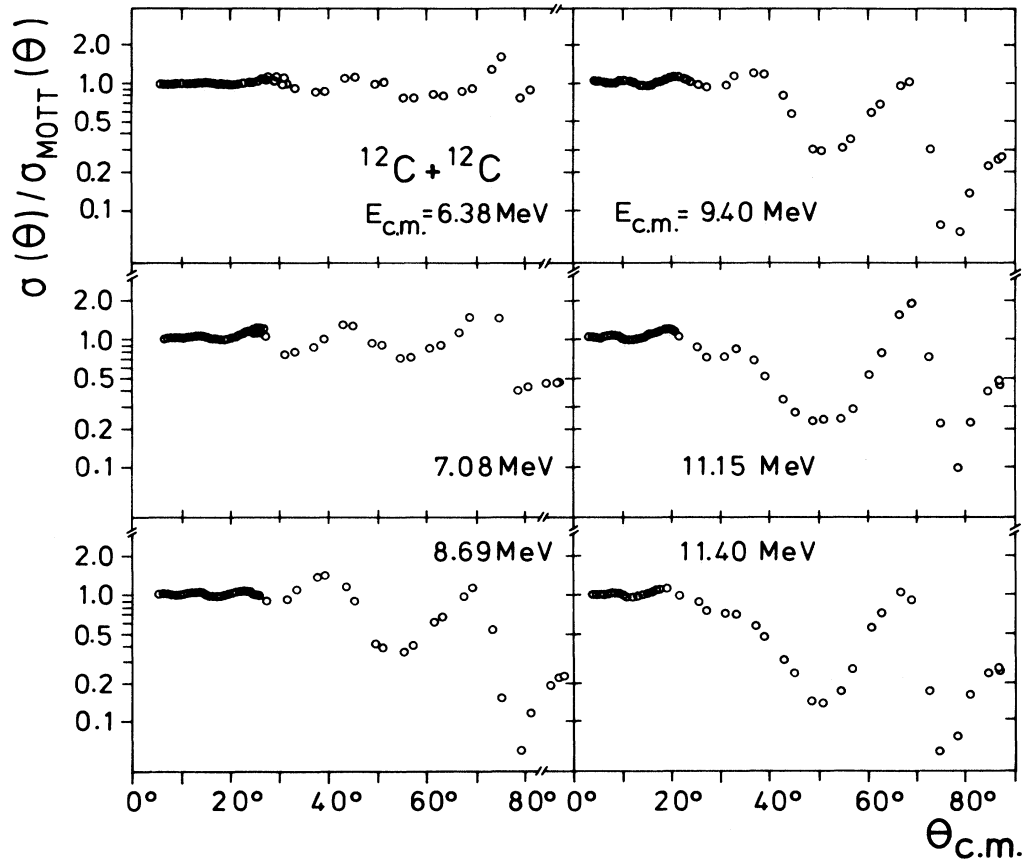

FIG. 10. Angular distributions of Fig. 9 with additional data points from Treu *et al.* [15].
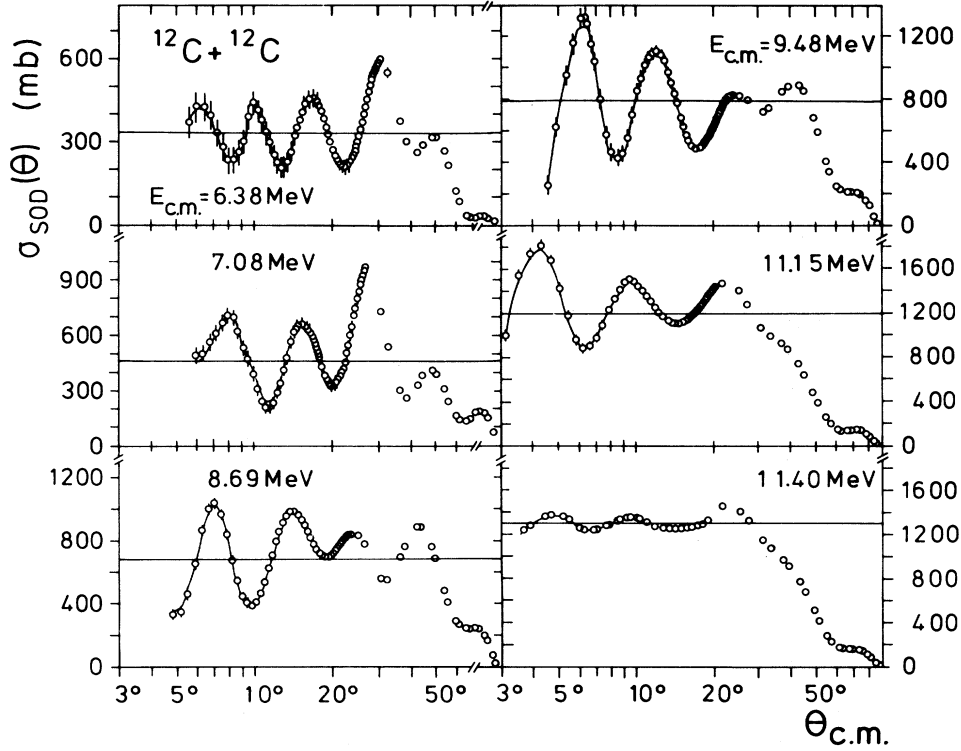
FIG. 11. Sum-of-differences cross sections obtained from the angular distributions of Fig. 10. The horizontal lines give the total reaction cross sections σ_R as obtained from χ^2 fits to the measured σ_{SOD} functions performed with approximation (7). The solid curves are the results of the χ^2 fits.

der of magnitude as the corresponding σ_R values shown as horizontal lines. This means that a forward nuclear glory exists in the $^{12}C + ^{12}C$ scattering for all energies investigated.

The additional fingerprint for a forward glory, i.e., undulating envelopes of the oscillating σ_{SOD} functions, are missing. This is to be expected in the present case due to the small values of the glory angular momenta ($l_g = 2-8$ in the energy range invesigated).

Quantitative values for $|f_N^s(\theta)|$ and σ_R were determined in a first step by means of approximation (8) as described in Sec. II (see Table I). The use of (8) is justified because one can expect, according to the investigation of the synthetic data (Sec. III A), that the experimental $\sigma_{SOD}(\theta_0)$ functions oscillate already with constant ampli-

tudes at the smallest angles measured.

The quantitative values for $4\pi|f_N^s(0)|/k$ confirm the above conclusion that a forward nuclear glory exists in the $^{12}C + ^{12}C$ scattering. Obviously the glory is considerably damped at the resonance.

The quantities $f_N^s(\theta)$ and σ_R were determined in addition by means of approximation (7) (with $\alpha = \theta_0$) because it was not clear a priori whether $\sigma_{SOD}(\theta_0)$ was indeed measured at angles small enough to justify the use of approximation (8). A χ^2 fit was performed to adjust approximation (7) to the measured $\sigma_{SOD}(\theta_0)$ function in the most forward angular range where (7) can be considered to be a good approximation ($\theta < \theta_g = 3\pi/l_g$, the angle of the first glory minimum of the semiclassical theory).

The start parameters for the χ^2 fit were $|f_N^s(0)|$, $\phi_N^s(0)$,

TABLE I. Quantities deduced from the measured $\sigma_{SOD}(\theta_0)$ functions by means of approximation (8). Errors as calculated according to Eq. (9) are given in parentheses. There is no safe procedure for the calculation of the errors on $\phi_N^s(0)$.

$E_{c.m.}$ (MeV)	σ_R (mb)	$|f_N^s(0)|$ (fm)	$\phi_N^s(0)$ (rad)	$4\pi|f_N^s(0)|/k$ (mb)
6.38	330(60)	1.3(0.2)	0.8	120
7.08	460(50)	3.1(0.3)	6.0	270
8.69	680(40)	4.8(0.3)	1.6	380
9.48	870(80)	6.6(0.6)	6.3	500
11.15	1350(50)	7.2(0.3)	6.3	500
11.38	1300(30)	1.3(0.2)	6.1	100

TABLE II. Quantities deduced from $\sigma_{SOD}(\theta_0)$ by means of approximation (7) with $\alpha=\theta_0$. The $|f_N^s(0)|$ values are obtained from an extrapolation of $|f_N^s(0)|$ values using relation (5); $\phi_N^s(0)$ values are obtained from a linear extrapolation.

$E_{c.m.}$ (MeV)	σ_R (mb)	$|f_N^s(0)|$ (fm)	$\phi_N^s(0)$ (rad)	$4\pi|f_N^s(0)|/k$ (mb)
6.38	330(60)	1.2(0.2)	0.8	110
7.08	460(50)	3.3(0.4)	6.0	290
8.69	680(40)	5.1(0.3)	1.6	410
9.48	790(80)	7.4(0.7)	6.2	560
11.15	1190(50)	6.6(0.3)	6.2	460
11.40	1290(30)	1.4(0.3)	6.0	100

and σ_R as determined with approximation (8); $|f_N^s(0)|$ was used, however, only for the angle θ' which corresponds to an extremum of σ_{SOD} observed at the smallest angles. For all other angles $|f_N^s(\theta_0)| = |f_N^s(0)|J_0(l_g\sin\theta)/J_0(l_g\sin\theta')$ was used as the start value. The fits were performed with two constraints: (i) $|f_N^s(\theta)|$ was allowed to vary only smoothly and (ii) σ_R had to be the same for all angles.

The results of the χ^2 fits are shown in Fig. 11 (solid curves) together with the σ_R values obtained simultaneously (horizontal lines). $|f_N^s(0)|$ values as extrapolated to $\theta=0°$ by means of Eq. (5) and $\phi_N^s(0)$ values obtained from a linear extrapolation are listed in Table II together with σ_R and $4\pi|f_N^s(0)|/k$ values. Again the $4\pi|f_N^s(0)|/k$ values represent a large fraction of the total reaction cross section σ_R. This again demonstrates that a nuclear glory exists in the $^{12}C+^{12}C$ scattering.

It is interesting to note that the values given in Tables I and II are nearly the same. This means that the conditions for the use of approximation (8) are indeed nearly fulfilled. Figure 12 shows $|f_N^s(\theta)|$ as a function of θ as determined from the χ^2 fit. The $|f_N^s(\theta)|$ values exhibit a $J_0(l_g\sin\theta)$ behavior as predicted by Eq. (5). This can be seen from a comparison with the $J_0(l_g\sin\theta)$ functions (solid lines in Fig. 12) calculated with glory angular momenta l_g which correspond to the grazing angular momenta. This angle dependence of $|f_N^s(\theta)|$ can be taken as additional proof for the existence of a nuclear glory in the $^{12}C+^{12}C$ scattering.

The $f_N^s(\theta)$ values determined in this work can be compared with values obtained from optical model calculations performed with the usual $^{12}C+^{12}C$ potentials. The comparison allows us eventually to identify the real potential among several potentials which describe the angular distributions equally well. This investigation is the subject of a forthcoming paper.

The σ_R values obtained in the present work are compared in Table III with σ_R values determined in Refs. [15], [27], and [28]. In Ref. [27] the α-particle, proton, and neutron yields of $^{12}C+^{12}C$ were summed up to get σ_R with an estimated error of 10%, in Ref. [28] the measured γ yield was equated with σ_R, and in Ref. [15] a special version of the GOT was used to deduce σ_R from elastic data with an error of 10%. Obviously the present σ_R values agree reasonably well with the values given in

Refs. [15] and [27] they exceed the values of Ref. [28] by a relatively large amount. This discrepancy is, most probably, due to the well known difficulty to find an absolute scale for cross sections determined from a γ-yield measurement.

Accurate σ_R values determined without using a model are important quantities for heavy-ion scattering systems. They impose an additional constraint on the determination of the scattering potential and allow, moreover, the evaluation of the elastic partial widths Γ_{el} of heavy-ion resonances [29]. The latter are necessary to establish the dinuclear structure of a resonance.

VII. CONCLUSION

It has been shown in this work that the sum-of-differences cross section $\sigma_{SOD}(\theta_0)$ exhibits exactly those features which were predicted in Refs. [5] and [12], i.e.,
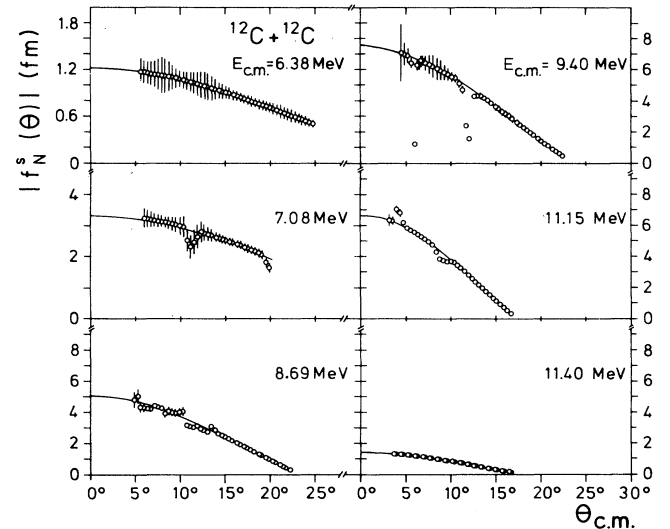

FIG. 12. $|f_N^s(\theta)|$ values obtained from a χ^2 fit to the measured σ_{SOD} curves. The solid lines represent Bessel functions $J_0(l_g\sin\theta)$ calculated with l_g values identical with the corresponding grazing angular momenta ($l_g=2$, 4, 6, 6, 8, and 8 for $E_{c.m.}=6.38$, 7.08, 8.69, 9.48, 11.15, and 11.40 MeV, respectively).

TALE III. Comparison of σ_R values for $^{12}C + ^{12}C$ determined in this work with previously published values. The numbers in parentheses denote the relative error quoted by the corresponding authors.

$E_{c.m.}$ (MeV)	σ_R (mb) This work	σ_R (mb) Ref. [15]	σ_R (mb) Ref. [27]	σ_R (mb) Ref. [28]
6.38	330(60)	327(33)	$\approx 200(20)$	
7.08	460(50)	461(46)	$\approx 400(40)$	
8.69	680(40)	907(91)	$\approx 750(75)$	450
9.48	790(80)	949(95)		510
11.15	1190(50)	999(100)		
11.40	1290(30)	1069(107)		

rapid oscillations at very forward angles which occur with constant amplitude for angles smaller than a critical angle. Moreover, it has been shown that $f_N^s(0)$ [or $f_N^s(\theta)$ at very forward angles] as well as σ_R can be deduced from $\sigma_{SOD}(\theta_0)$ in a model-independent way with good accuracy. The fact that $4\pi |f_N^s(0)|/k$ represents a large fraction of the total reaction cross section σ_R is evidence of the existence of a forward nuclear glory in the $^{12}C + ^{12}C$ system. This is the first time that a forward nuclear glory has been observed in a heavy-ion scattering system based on real experimental data.

To obtain this information it was, however, necessary to measure elastic angular distributions with high precision up to very small scattering angles. This unusual accuracy, particularly at very forward angles, prevents this type of experiment most probably from being carried out routinely for the determination of σ_R and $f_N(0)$. It is only possible to perform such experiments in a few selected cases. The results which can be obtained are suited to disentangle ambiguities in equivalent potentials, to evaluate elastic partial widths in case of heavy-ion resonances, and to deduce accurate phase shifts needed for the investigation of the inverse scattering problem.

ACKNOWLEDGMENTS

*Present address: Siemens AG, D-8520 Erlangen, Germany.

[1] H. M. Nussenzveig and W. J. Wiscombe, Opt. Lett. **5**, 455 (1980).

[2] R. B. Bernstein, J. Chem. Phys. **34**, 361 (1961).

[3] E. W. Rother, P. K. Rol, S. M. Trujillo, and R. H. Neynaber, Phys. Rev. **128**, 659 (1962).

[4] M. S. Hussein, H. M. Nussenzveig, A. C. C. Villari, and J. L. Cardoso, Phys. Lett. **114B**, 1 (1982).

[5] J. Barrette and N. Alamanos, Phys. Lett. **153B**, 208 (1985); Nucl. Phys. **A441**, 733 (1985).

[6] W. Tiereth, Z. Basrak, N. Bischof, B. Nees, E. Nieschler, I. Weitzenfelder, and H. Voit, Nucl. Phys. **A464**, 125 (1987).

[7] V. Hnizdo, Phys. Lett. **167B**, 26 (1986).

[8] A. Ostrowski, W. Tiereth, D. Brandl, Z. Basrak, and H. Voit, Phys. Lett. B **232**, 46 (1989).

[9] K. W. Ford and J. A. Wheeler, Ann. Phys. (N.Y.) **7**, 259 (1959).

[10] R. B. Bernstein, in *Molecular Beams*, edited by J. Ross, Adv. Chem. Phys. Vol. X (Wiley, New York, 1966), p. 75.

[11] J. T. Holdeman and R. M. Thaler, Phys. Rev. Lett. **14**, 81 (1965); Phys. Rev. **139**, B1186 (1965).

[12] C. Marty, Z. Phys. A **309**, 261 (1983).

[13] R. Lipperheide, Nucl. Phys. **A469**, 190 (1987).

[14] M. S. Hussein, A. Lépine-Szily, M. M. Saad, and A.C.C. Villari, Phys. Rev. Lett. **52**, 511 (1984).

[15] W. Treu, H. Fröhlich, W. Galster, P. Dück, and H. Voit, Phys. Rev. C **22**, 2462 (1980).

[16] C. Marty, Z. Phys. A **322**, 499 (1985).

[17] D. C. Carey, Nucl. Instrum. Methods **104**, 173 (1972).

[18] W. R. Kuhlmann, K. H. Lauterjung, B. Schimmer, and K. Sistemich, Nucl. Instrum. Methods **40**, 118 (1966).

[19] H. Voit, W. Galster, W. Treu, H. Fröhlich, and P. Dück, Phys. Lett. **67B**, 399 (1977).

[20] W. Galster, Ph.D. thesis, University Erlangen-Nürnberg, 1977.

[21] D. Vetterli, P. Egelhof, G. Baur, W. Boeglin, R. Henneck, A. Klein, H. Muehig, G. R. Plattner, F. Roesel, I. Sick, D. Trautmann, A. Weller, and M. Yaskola, in *Weak and Electromagnetic Interactions in Nuclei*, Proceedings of the International Symposium, Heidelberg, West Germany, 1986, edited by H. V. Klapdor (Springer, New York, 1987), p. 105.

[22] H. J. Assenbaum, K. Langanke, and C. Rolfs, Z. Phys. A **327**, 461 (1987).

[23] J. D. Jackson, *Classical Electrodynamics* (Wiley, New York, 1975).

[24] E. A. Uehling, Phys. Rev. **48**, 55 (1935).

[25] H. Akima, ACM Trans. Math. Software **4**, 148 (1978).

[26] R. Giordano, F. Porto, S. Sambataro, and A. Scalia, Nuovo Cimento **A61**, 182 (1981).

[27] J. R. Patterson, H. Winkler, and C. S. Zaidins, Astrophys. J. **157**, 367 (1969).

[28] K. A. Erb, R. R. Betts, S. K. Korotky, M. M. Hindi, P. P. Tung, M. W. Sachs, S. J. Willet, and D. A. Bromley, Phys. Rev. C **22**, 507 (1980).

[29] W. Treu, H. Fröhlich, P. Dück, and H. Voit, Phys. Rev. C **28**, 237 (1983).